Supplementary Figure 1: Fly holder for 40x and 60x objective

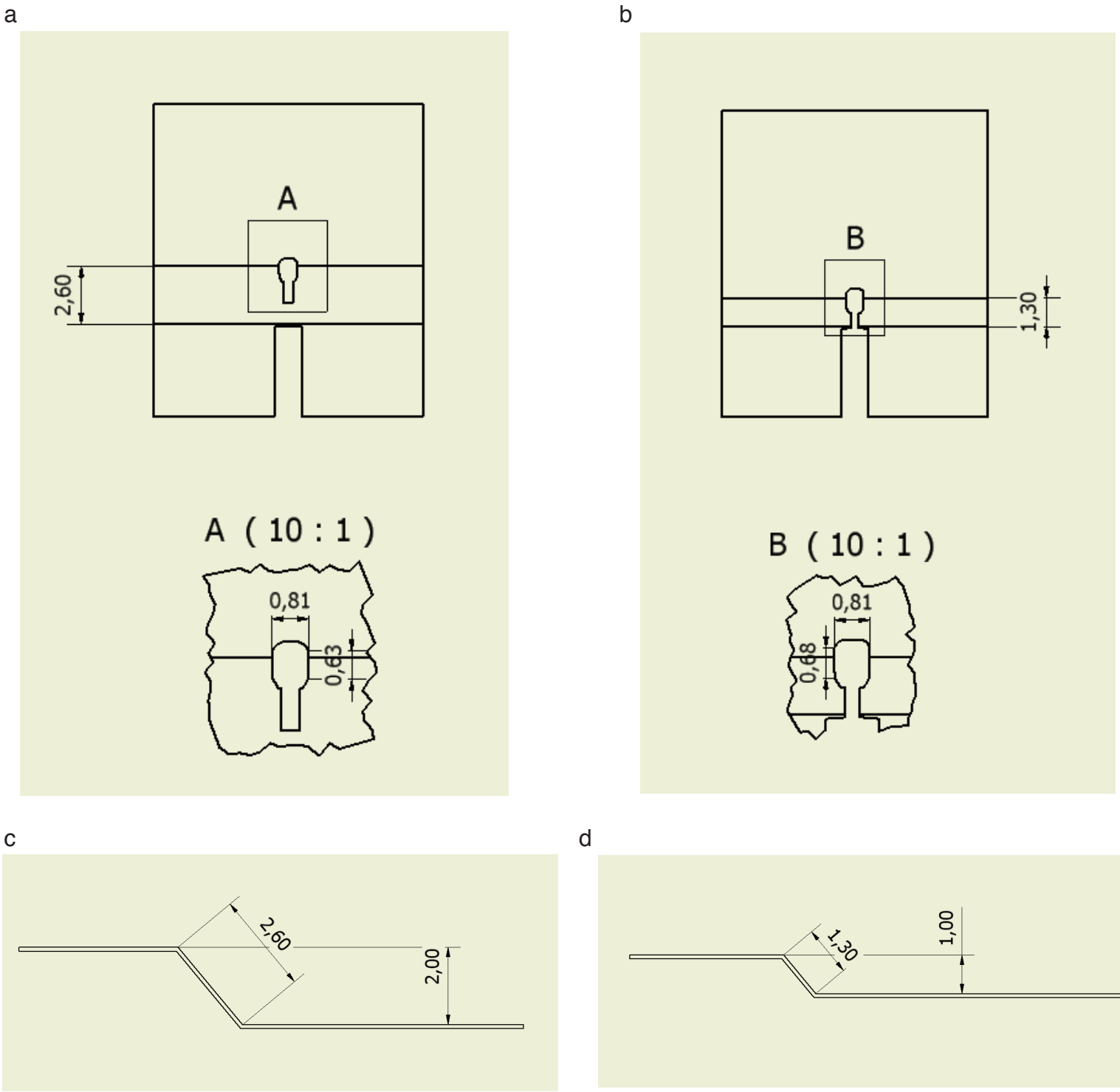

Fly holder. a. For 40X and b. for 60X objectives. A laser mill is used to cut grooves in stainless steel shim along the lines shown. Shim is then folded twice along the grooves (indicated by arrows) to create a step (c and d for 40X and 60X respectively) that provides the objective with working distance to image the brain while keeping the fly's body sufficiently free.

Supplementary Figure 2: Fly holder, dissection and positioning

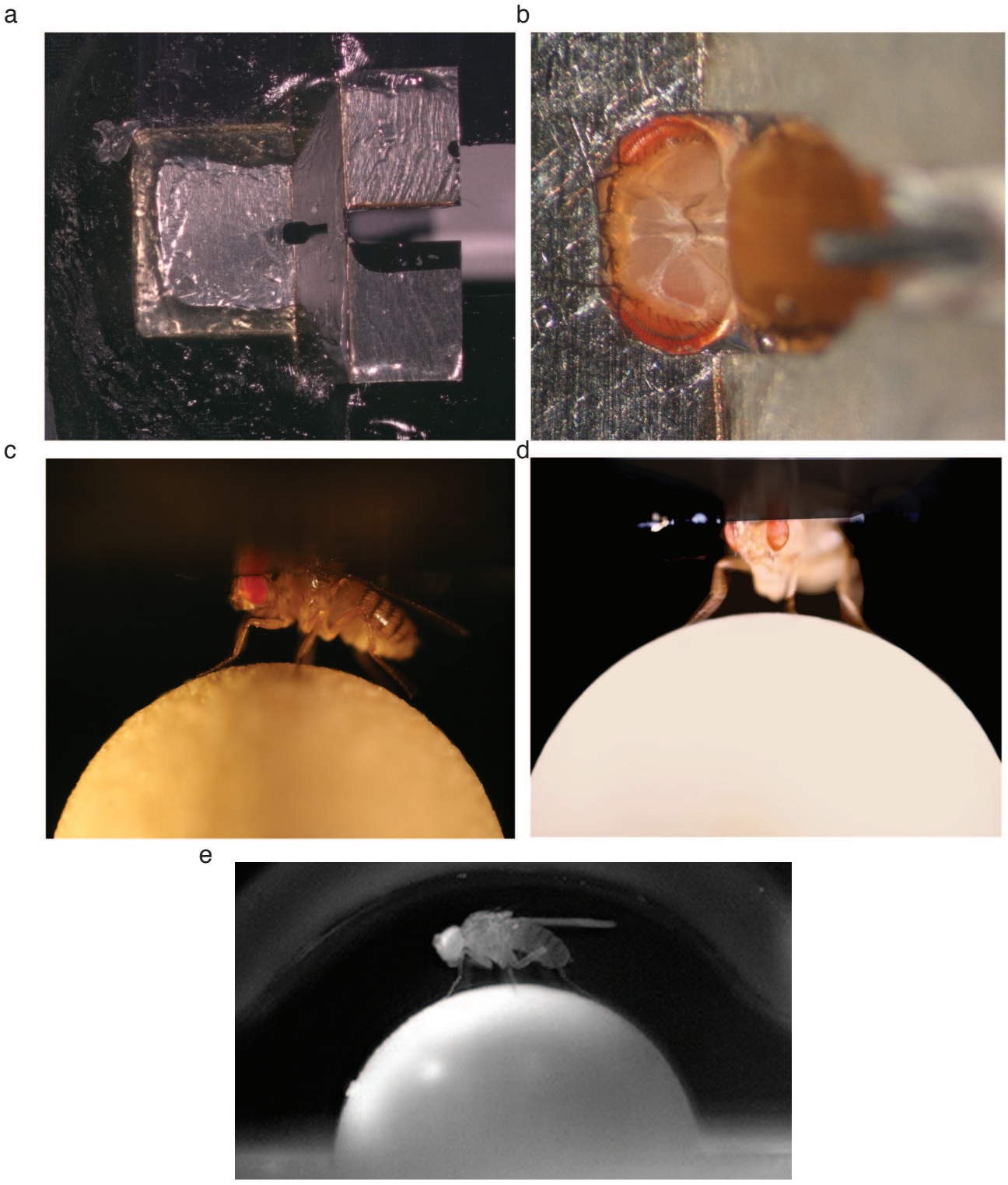

a. Top view of the fly holder. b. Top view of the fly head with cuticle removed. The pin glued to the fly's thorax during mounting is also visible at right. c. Side and d. frontal views of the head-fixed fly mounted on the holder and standing on the ball under recording conditions. e. Side view of a free-walking fly on a 6-mm diameter curved surface.

Supplementary Figure 3: Bleedthrough-induced fluorescence caused by the arena

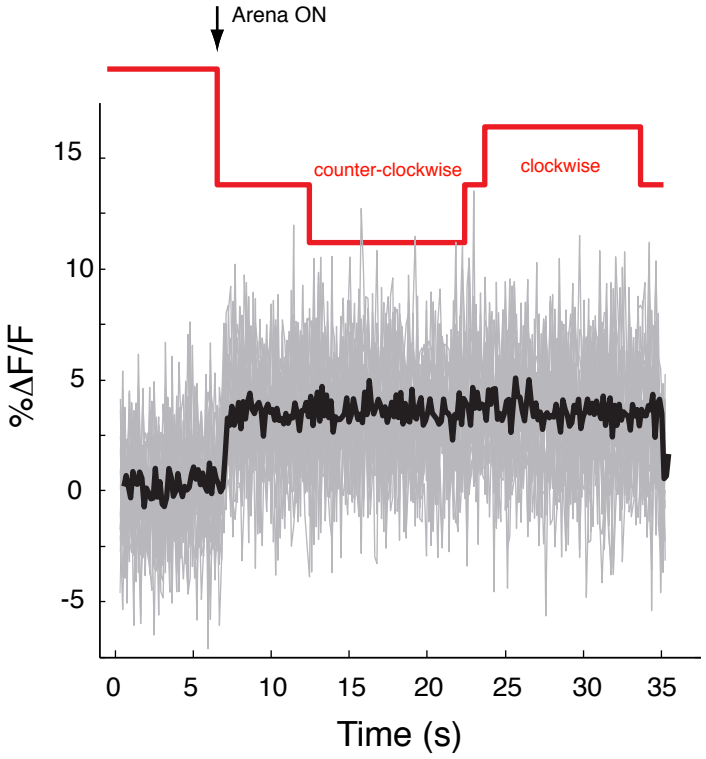

We computed the change in fluorescence (%ΔF/F) in a region of the field of view with no GCaMP expression (i.e., background) with respect to a fluorescence baseline calculated with the arena off. Highlighted in red is the arena signal of a typical experiment, which contained patterns moving clockwise and counter-clockwise at the indicated times. The arena was turned on with the stationary pattern.

Supplementary Figure 4: Walking performance of head-fixed flies

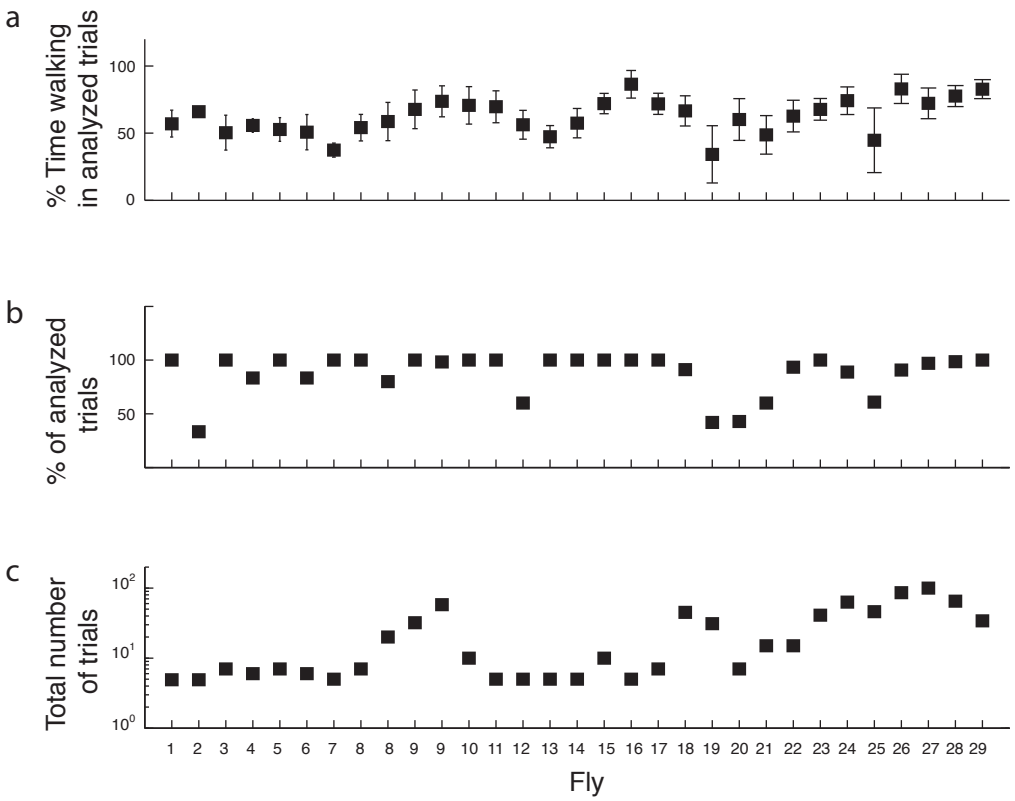

a. Average time spent walking during PD and ND stimulation per fly in trials where flies walked more than 30% of the time. b. Proportion of trials that reached the threshold criteria for analysis (walking > 30% of the time). c. Total number of trials per fly.

Supplementary Figure 5: Optomotor index and calcium transients depend on visual stimulation

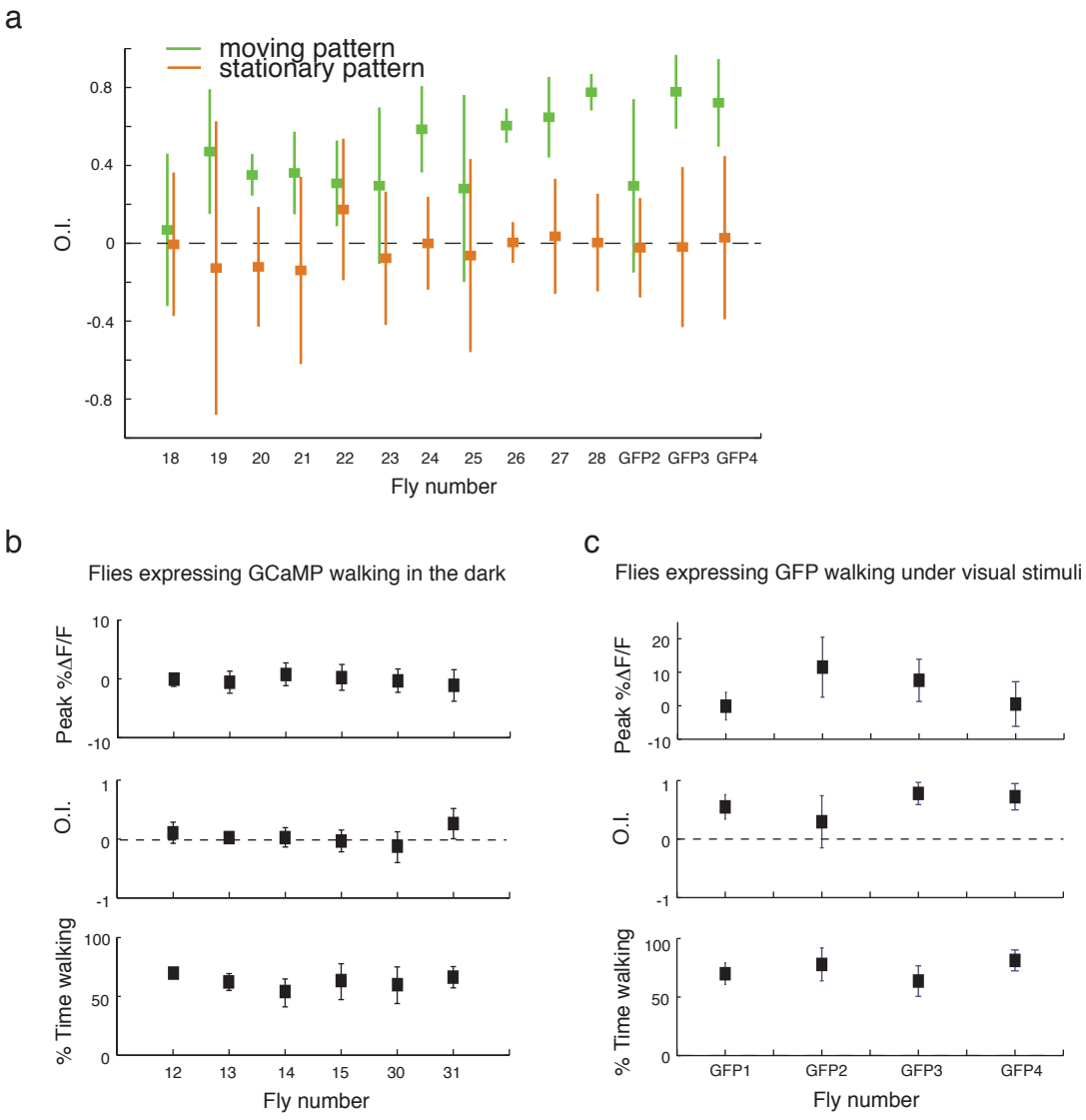

a. Optomotor behavior under moving (red) or stationary (blue) grating. Mean O.I. for motion stimuli = 0.53 ± 0.014 and mean O.I. for stationary patterns = -0.0041 ± 0.0137, significantly different (p = 8.4*10-106, Mann-Whitney). b. Calcium signals (top), optomotor behavior (middle) and percentage of walking (bottom) in flies expressing GCaMP walking in the dark, i.e., with no visual stimulus. c. Same, for flies expressing GFP.

Supplementary Figure 6: Walking and optomotor performance in free-walking flies

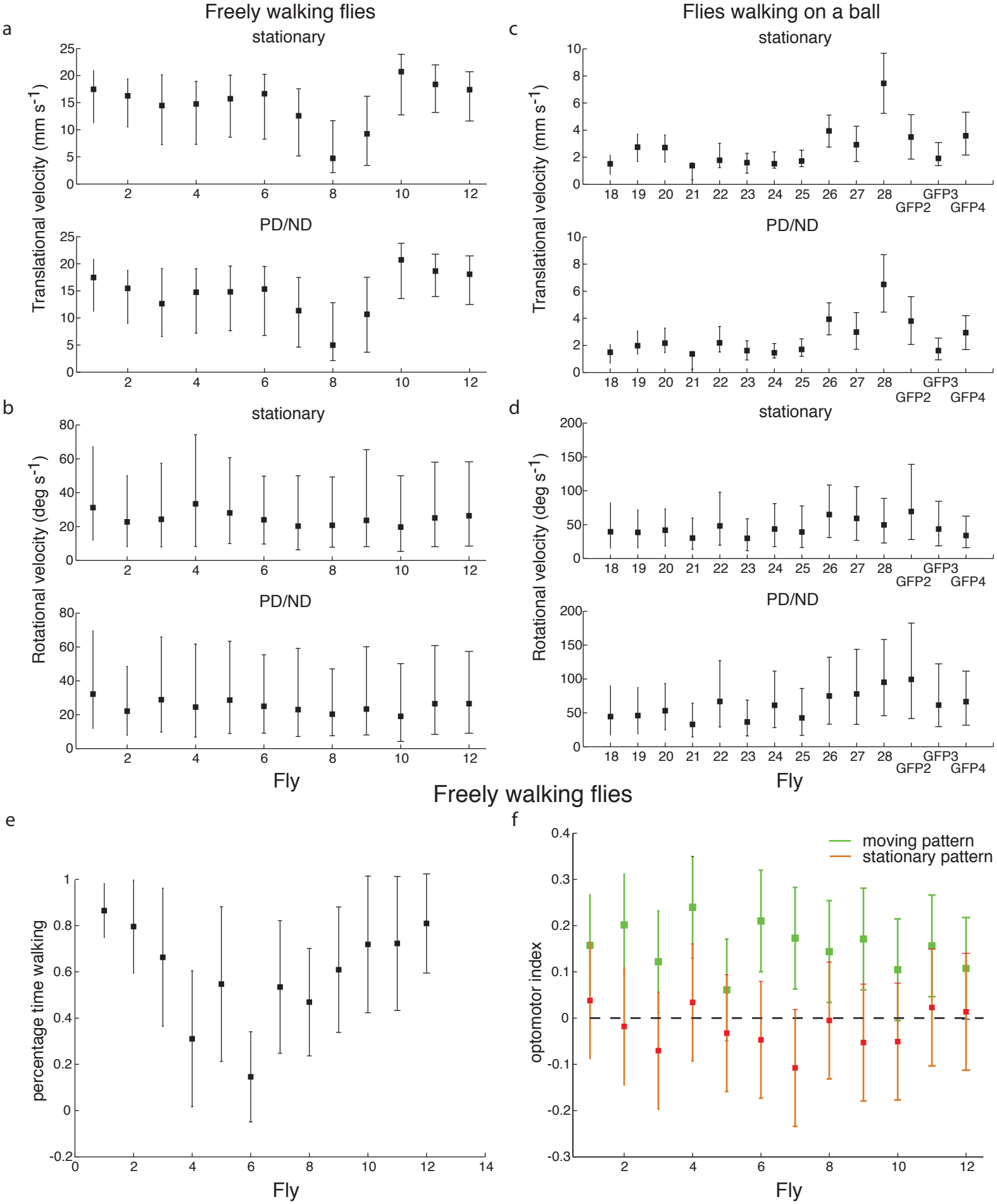

a., b. Translational and rotational velocities of free-walking flies under stationary and moving pattern stimulation. c, d. Same for tethered flies on a ball. e. Percentage of walking (translational velocities > 1 mm/s) in freely walking flies. f. Optomotor indices for freely walking flies under stationary and motion pattern visual stimulation. Compare to Supplementary Fig. 5a showing similar plot for tethered walking flies.

Supplementary Figure 7: Stability of fluorescence signal and fly walking performance over time

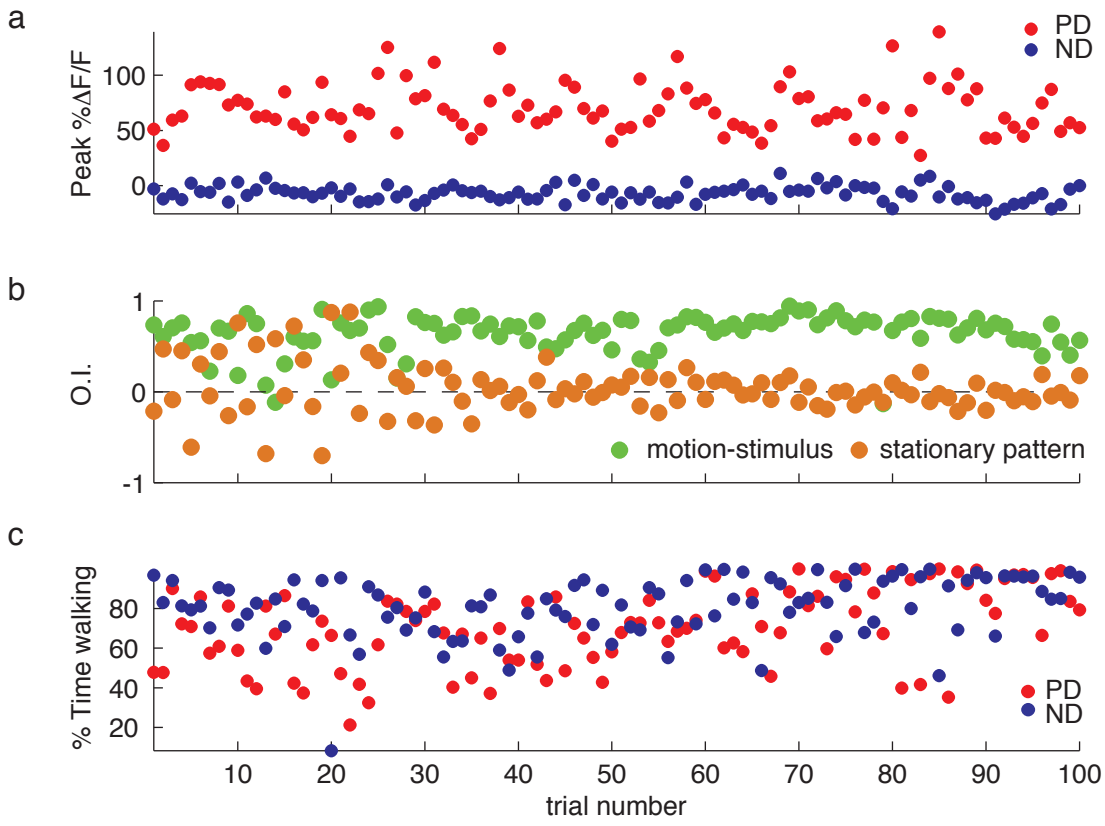

Example of Fly 27 walking performance during PD (red) or ND (blue) segments across all trials. a. Calcium signal. b. Optomotor index (O.I.); green: response to motion stimulus, orange: response to stationary pattern. c. Percentage of walking per trial.

Supplementary Figure 8: Schematics for the ball holder and ball file

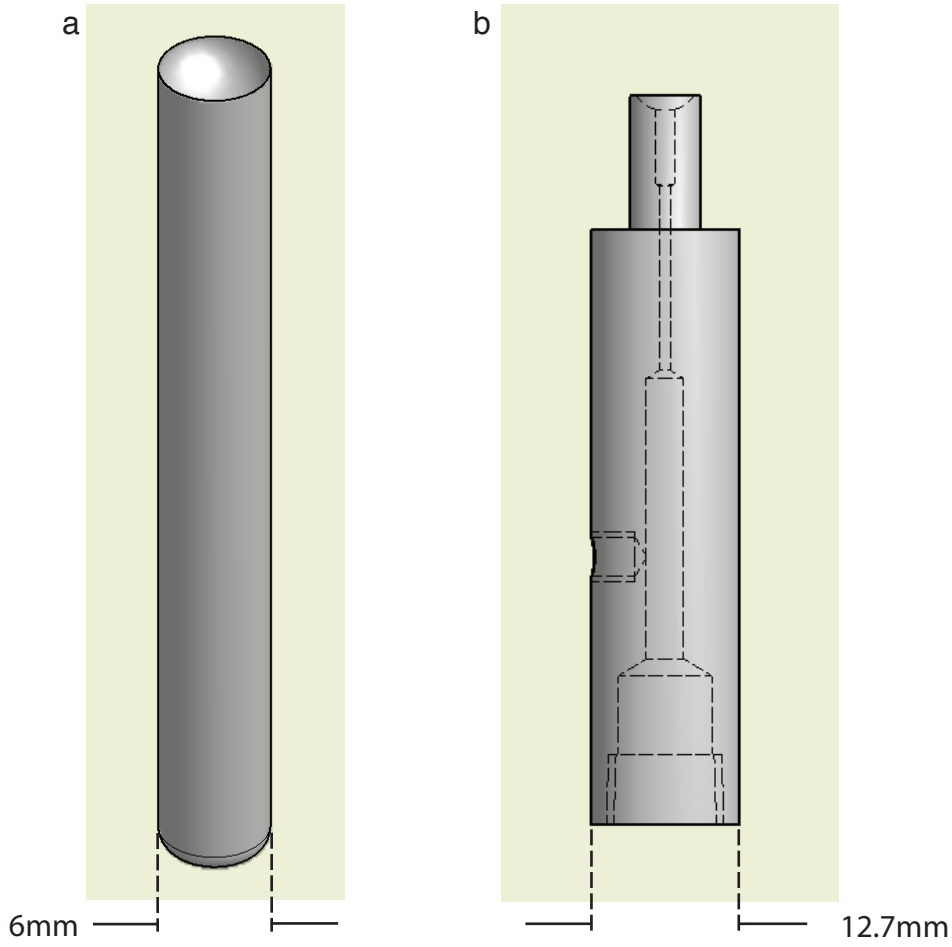

a. Drawing of ball file used for making balls. b. Drawing of ball holder.

Supplementary Figure 9: Ball tracker system block diagram

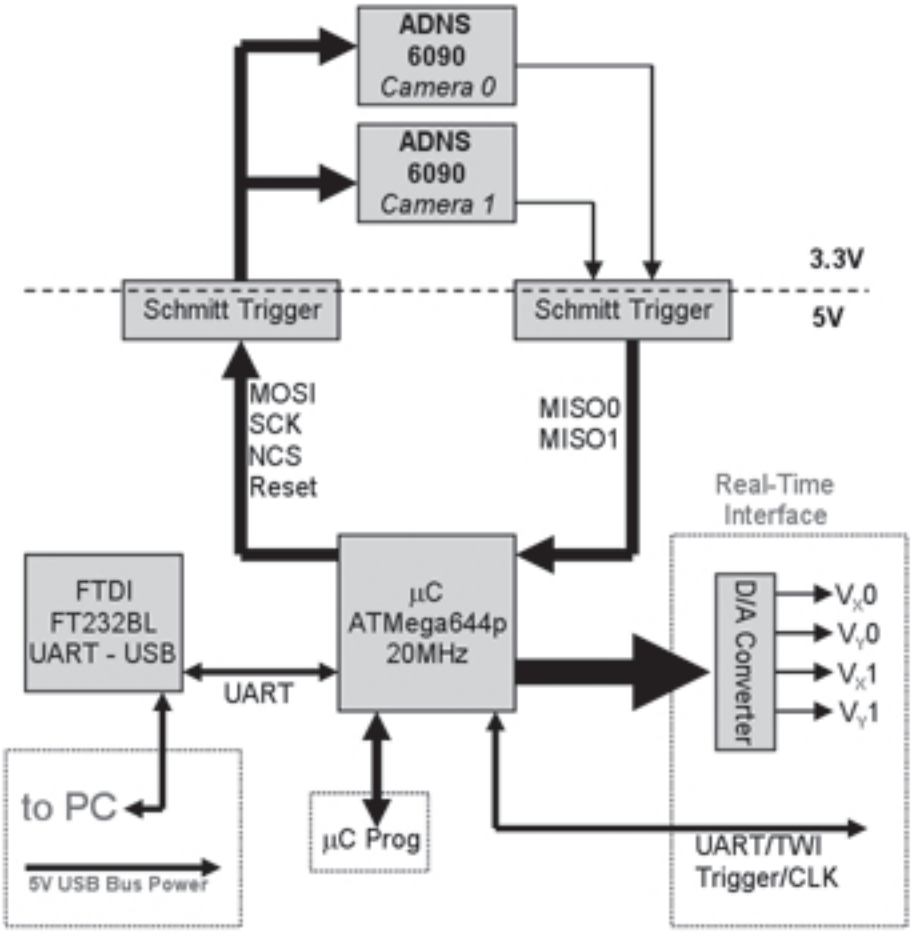

The device consists of two optical mouse sensor chips (ADNS-6090), a master microcontroller running at 20 MHz (ATMega644p), a digital/analog deterministic status interface, and a USB connection to a PC based system for control, calibration, and data logging. The firmware program is uploaded via an in-system programmer.

Supplementary Figure 10: Tracking system camera housing

a

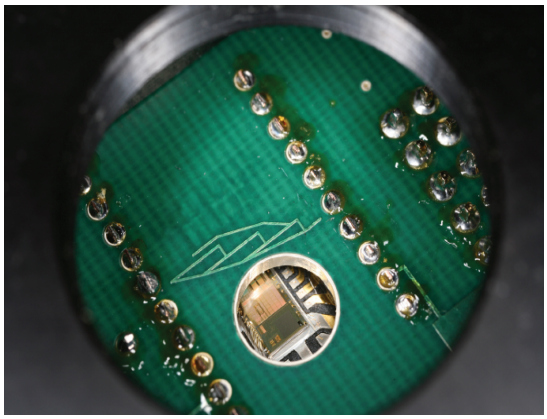

b

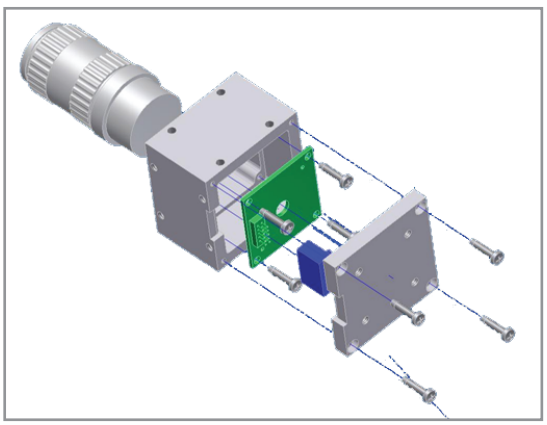

a. View of the PCB through the lens thread, showing the exposed optical flow ASIC (ADNS-6090). This ASIC is capable of 4 kHz measurements of optical flow by sequential image frame correlation. An integrated plastic bushing delivered with the device is removed to expose the 30x30 pixel array and the chip is pressed flush against the backside of a printed circuit board. A face of a 6 mm ball treadmill is projected onto the optical flow sensor's photoactive elements by modular optics. b. This exploded view of one of the two camera housings illustrates our adaptation of arbitrary c-mount optics to the optical mouse sensor system. The housing dimensions are 1.85x1.85x1.5 in and the optical flow sensor is mounted at the center of the lens thread with a flange focal length of 0.69 in. Several standard □-20 thread mounting holes are integrated into the case to facilitate mounting in the experimental apparatus.

Supplementary Figure 11: Calibration of the tracking system

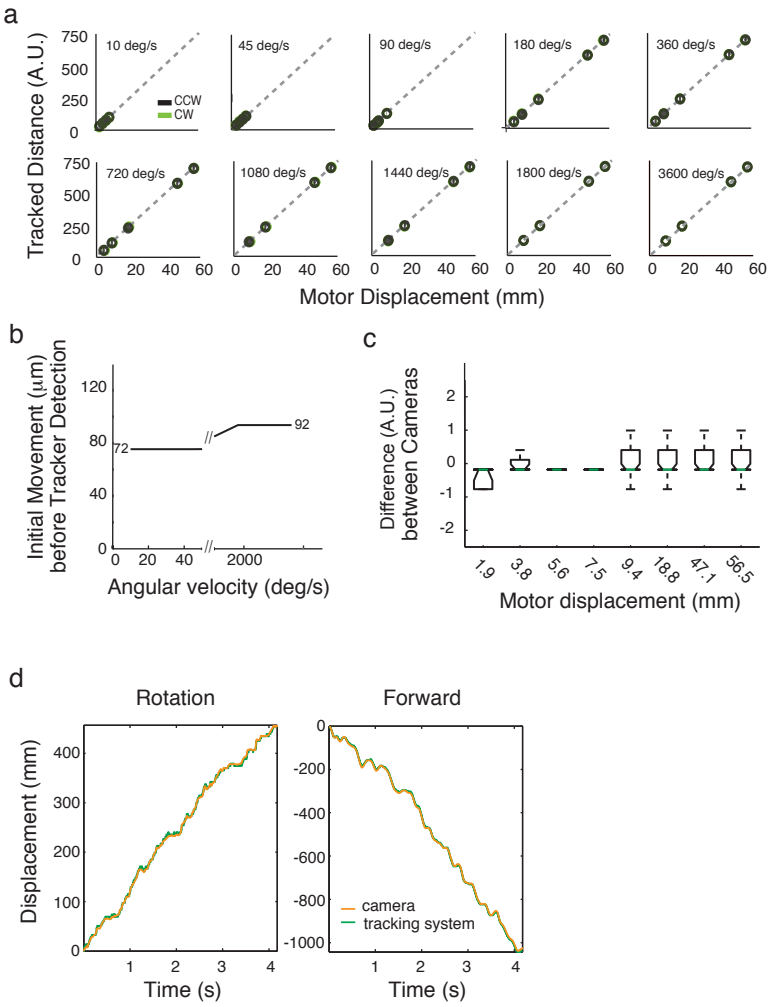

a. A 6-mm ball mounted on a motor was rotated clockwise and counter-clockwise at different velocities. Tracked movements (arbitrary units, A.U.) were compared to actual displacements. b. The precision of the system is evaluated by plotting the initial amount of movement before tracker detection, as a function of different velocities of rotation. c. Difference in the tracked motion between the two cameras (n= 40 trials). d. Ball displacements as measured by the tracking system (green) were compared to ball displacements computed by measuring optic flow in 480 Hz video images of the ball (orange). Shown are rotation and forward displacements of the ball.

a

Supplementary Figure 12: Setup for flies walking on a ball in visual arena

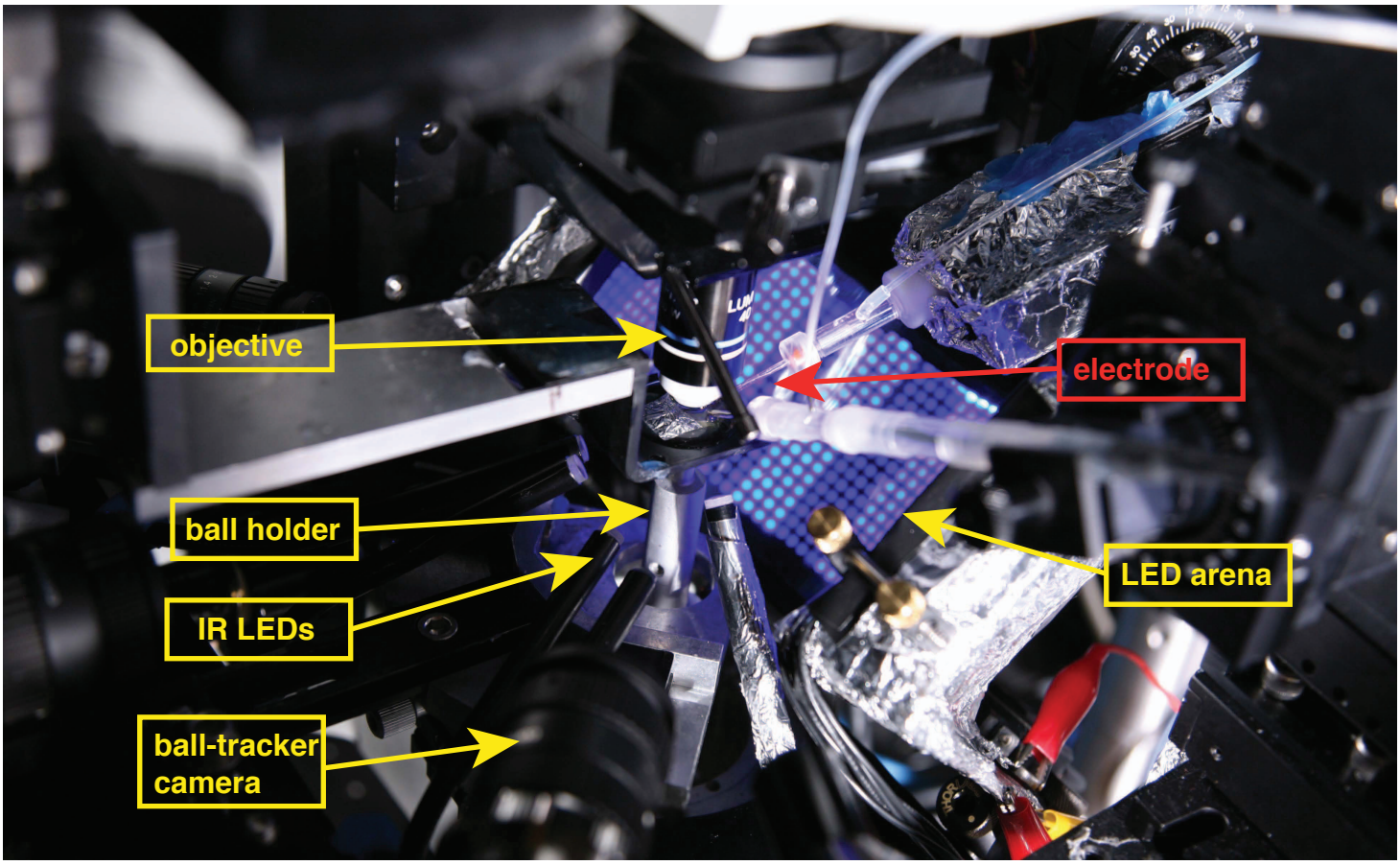

b

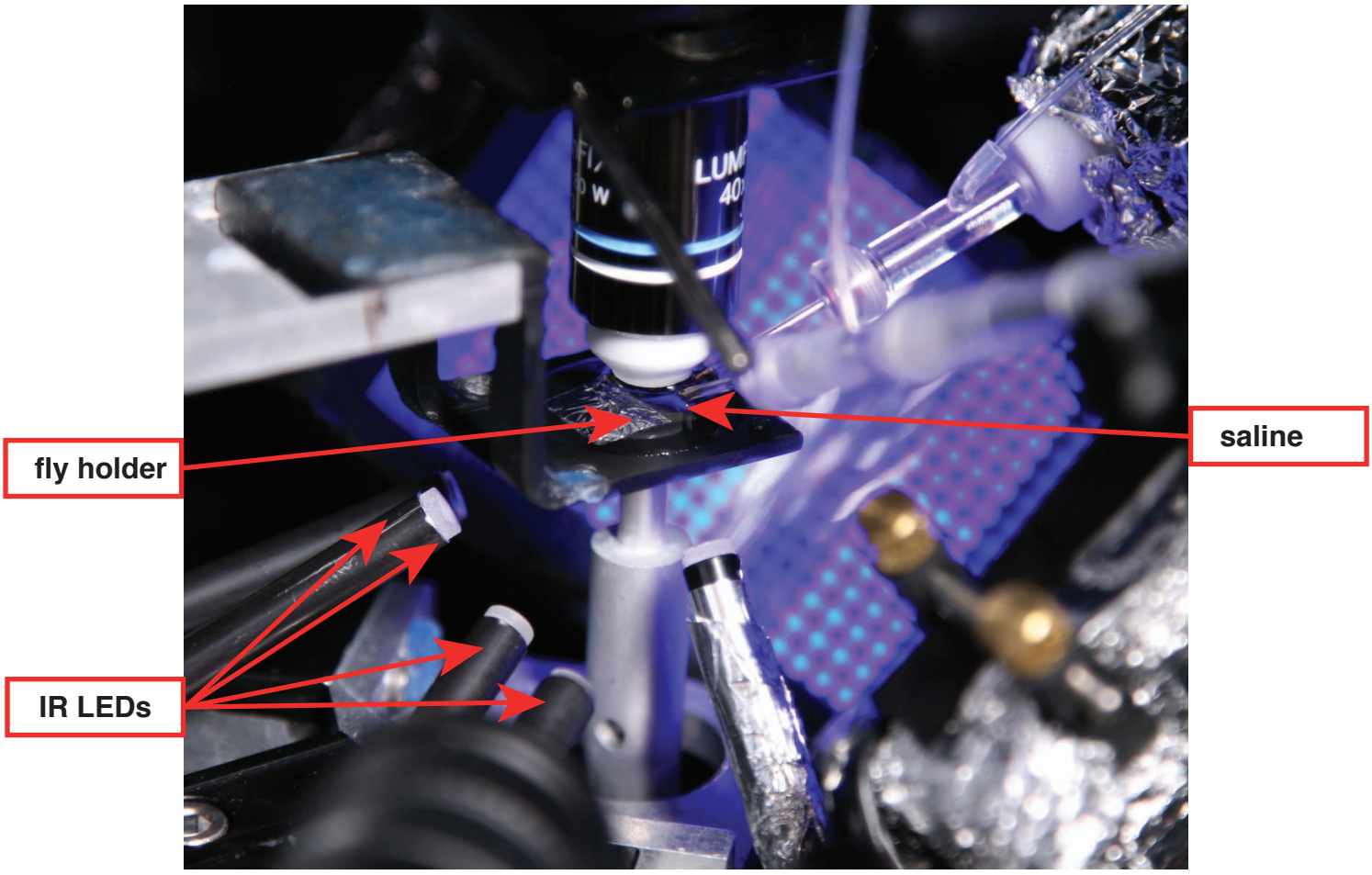

a. Photograph of the fly-on-a-ball rig. b. A zoomed in view showing positioning of the fly holder, ball holder, and IR LEDs.

Supplementary Figure 13: Histograms of motion corrections over all frames and trials

a

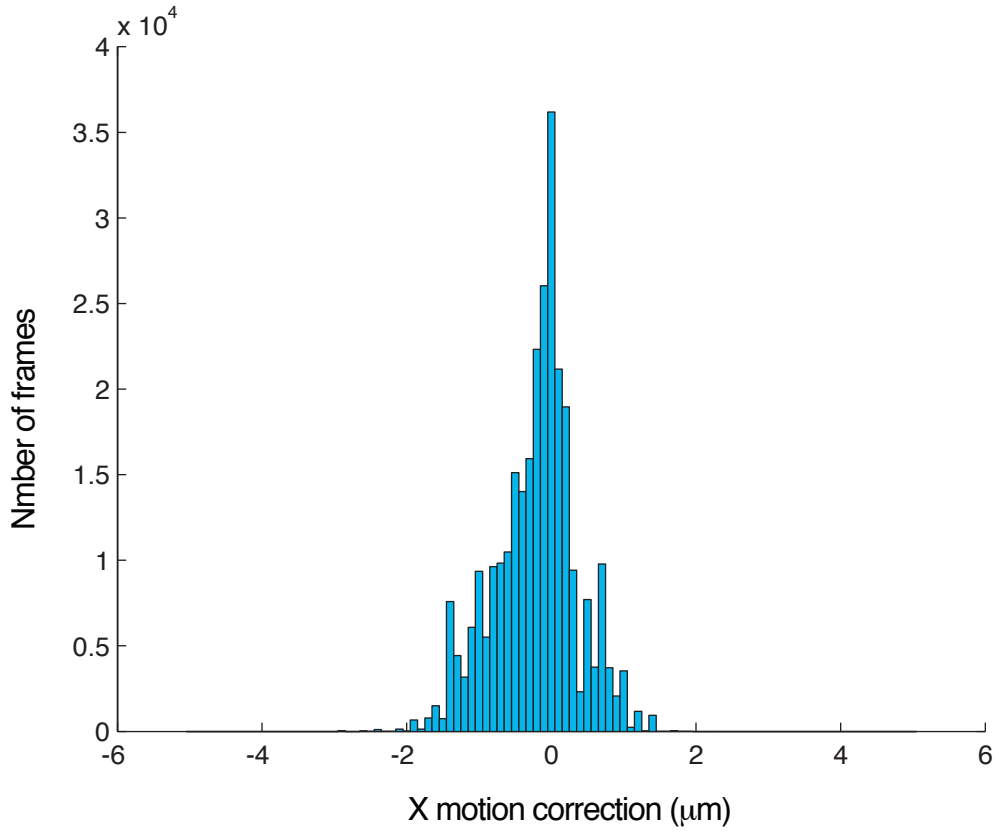

b

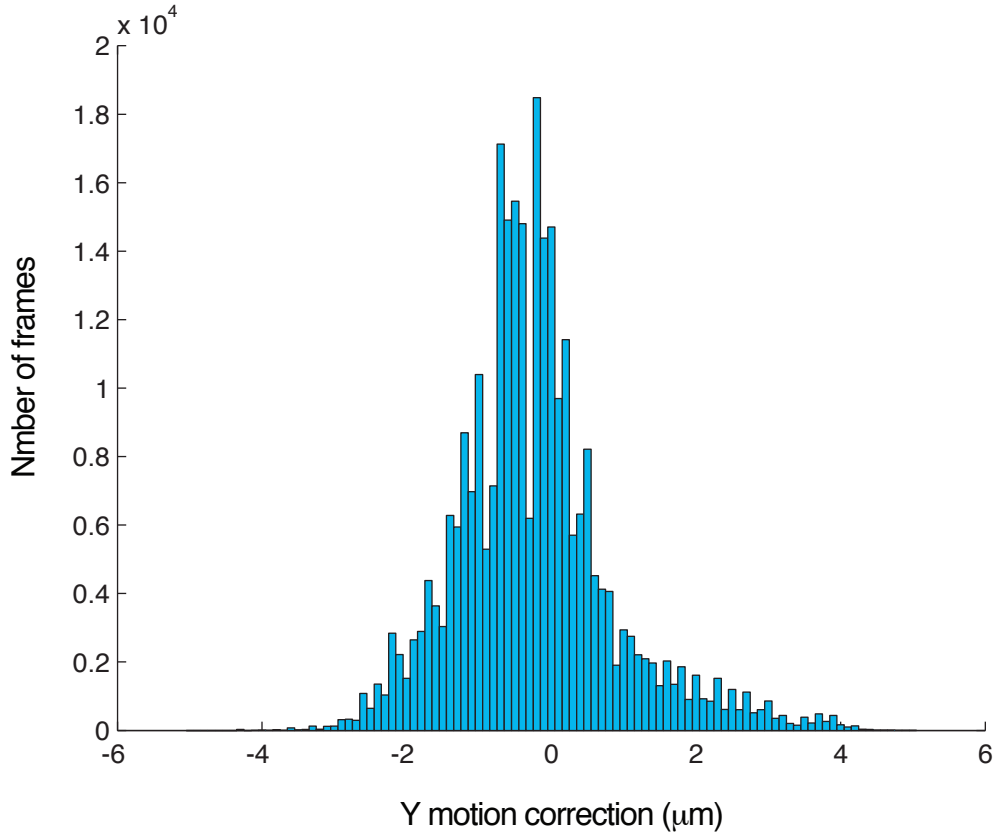

a. X motion correction: 0.45 ± 0.41 μm. b. Y motion correction: 0.84 ± 0.74 μm. Both: mean ± s.d. of absolute value of motion corrections.

Supplementary Information for Fig. 4.

Fig. 4g-h. Numbers and statistics.
For Fig. 4g, numbers of trials with positive versus negative correlations were (for Fly 18-28 respectively): 19/6, 12/0, 3/0, 8/0, 8/3, 27/4, 54/0, 17/2, 78/0, 81/14, 63/1.
For Fig. 4h, p-values for t-test for lag distributions being significantly different from normal distribution around 0: $6*10^{-5}$, 0.0075, 0.27, 0.01, $4*10^{-10}$, $6*10^{-17}$, $3*10^{-4}$, $4*10^{-6}$, $7*10^{-13}$, $2*10^{-27}$.

Supplementary Movies
Note: The xvid codec is required to play all movies.